[CANCER RESEARCH 63, 354–363, January 15, 2003]

A Universal Pretargeting System for Cancer Detection and Therapy Using Bispecific Antibody[1]

Robert M. Sharkey,[2] William J. McBride, Habibe Karacay, Ken Chang, Gary L. Griffiths, Hans J. Hansen, and David M. Goldenberg

Center for Molecular Medicine and Immunology, Belleville, New Jersey 07109 [R. M. S., H. K., D. M. G.]; Immunomedics, Inc., Morris Plains, New Jersey 07950 [W. J. M., K. C., G. L. G., H. J. H., D. M. G.]; and IBC Pharmaceuticals, Inc., Morris Plains, New Jersey 07950 [K. C., D. M. G.]

ABSTRACT

Multistep targeting systems represent highly selective alternatives to targeting systems using directly radiolabeled antibodies for diagnostic and therapeutic applications. A flexible bispecific antibody (bsMAb) multistep, pretargeting system that potentially can be developed for use with a variety of different imaging or therapeutic agents is described herein. The flexibility of this system is based on use of an antibody directed against histamine-succinyl-glycine (HSG) and the development of peptides containing the HSG residue. HSG-containing peptides were synthesized with either 1,4,7,10-tetraazacyclododecane-*N,N′,N″,N‴*-tetraacetic acid for the chelation of ^{111}In, ^{90}Y, or ^{177}Lu, or a technetium/rhenium chelate. The peptides can be radiolabeled to a high specific activity in a facile manner that avoids the need for purification. *In vivo* studies in nude mice bearing human colon tumor xenografts showed that the radiolabeled peptides cleared rapidly from the body with minimal retention in tumor or normal tissues. For pretargeting, these peptides were used in combination with a bsMAb composed of the anti-HSG Fab′ that was covalently coupled with the Fab′ of either an anticarcinoembryonic antigen or an anticolon-specific antigen-p antibody to provide tumor targeting capability. When the radiolabeled peptides were administered 1–2 days after a pretargeting dose of the bsMAbs, tumor uptake of the radiolabeled peptides increased as much as 28–175-fold over that seen with the peptides alone with tumor:nontumor ratios exceeding 2:1 to 8:1 within just 3 h of the peptide injection, which was a marked improvement over the tumor:nontumor ratios seen with a directly radiolabeled ^{99m}Tc-anti- anticarcinoembryonic antigen Fab′ at this same time. The anticolon-specific antigen-p x anti-HSG F(ab′)$_2$ bsMAb had the highest and longest retention in the tumor, and when used in combination with the ^{111}In-labeled peptide, radiation dose estimates for therapeutic radionuclides, such as ^{90}Y and ^{177}Lu, suggested that antitumor effects would be expected with tolerable radiation exposure to the normal tissues. These results suggest that this multistep, pretargeting system has diagnostic imaging and therapeutic potential.

INTRODUCTION

Multistep, pretargeting methodologies have received considerable attention for cancer imaging and therapy (1, 2). Unlike direct targeting systems, where an effector molecule (*e.g.*, a radionuclide or a drug linked to a low molecular weight carrier) is directly linked to the targeting agent, in pretargeting systems, the effector molecule is given some time after the targeting agent (1, 2). This allows time for the targeting agent to localize in tumor lesions and, more importantly, clear from the body. Because most targeting agents have been antibody proteins, they tend to clear much more slowly from the body (usually days) than the low molecular weight effector molecules (usually in min). In direct targeting systems involving therapeutic radionuclides, the body, and in particular the highly vulnerable red marrow, is exposed to the radiation during the period when the targeting agent is slowly reaching its peak levels in the tumor and clearing from the body. In a pretargeting system, the radionuclide is usually bound to a low molecular weight "effector" molecule, such as a chelate or peptide, which clears very quickly from the body. Thus exposure of normal tissues is minimized. Maximum tumor uptake of the radionuclide occurs very rapidly, because the low molecular weight molecule efficiently traverses the tumor vasculature and binds to the primary targeting agent. Its small size may also encourage a more uniform distribution in the tumor (3).

Pretargeting methods have used a number of different strategies, but most often have involved an avidin/streptavidin-biotin or bsMAbs recognition system (1, 2, 4–9). The avidin/streptavidin system is highly versatile and has been used in several configurations. Antibodies can be coupled with streptavidin or biotin, which is used as the primary targeting agent (4, 6). This is followed sometime later by the effector molecule, which is conjugated with biotin or with avidin/streptavidin, respectively. Another configuration relies on a three-step approach first targeting a biotin-conjugated antibody, followed by a bridging with streptavidin/avidin, and then the biotin-conjugated effector is given (5). Each of these systems is optimized by including a clearing/blocking step to remove the antibody conjugate from the blood (4–6). Without this step, the antibody conjugate in the blood would take up the majority of the effector, thereby reducing tumor uptake and T:NTs for the effector. These systems can be converted for use with a variety of effector substances so long as the effector and the targeting agent can be coupled with biotin or streptavidin/avidin, depending on the configuration to be used. With its versatility and high binding affinity between avidin/streptavidin and biotin, this type of pretargeting has considerable advantages over other proposed systems. However, avidin and streptavidin are foreign proteins and, therefore, would be immunogenic, which would limit the number of times they could be given in a clinical application. In this respect, bsMAbs[3] have the potential advantage of being engineered as relatively nonimmunogenic humanized proteins. The extremely high affinity of the streptavidin/avidin-biotin affinity ($\sim 10^{-15}$ M) has also been cited as major advantage of these systems. In addition, avidin has up to four binding sites for biotin that provide greater avidity. In this regard, since most bsMAbs have had only one arm for capturing the effector, the binding affinity (typically 10^{-9}–10^{-10} M) and avidity for a bsMAb are significantly lower than avidin-biotin. However, because both pretargeting systems are dependent on the binding affinity of the primary targeting agent (*i.e.*, the antibody binding to the tumor antigen), the higher affinity and avidity of streptavidin/avidin for biotin may not be a substantial advantage over a bsMAb pretargeting system, because the effectors in both systems will be anchored to the tumor by

Received 2/13/02; accepted 11/14/02.

The costs of publication of this article were defrayed in part by the payment of page charges. This article must therefore be hereby marked *advertisement* in accordance with 18 U.S.C. Section 1734 solely to indicate this fact.

[1] Supported in part by United States Department of Energy grant DE-FG01-00NE22941 and PHS grant CA81760 from the NCI.

[2] To whom requests for reprints should be addressed, at Center for Molecular Medicine and Immunology, 520 Belleville Avenue, Belleville, NJ 07109. Phone: (973) 844-7121; Fax: (973) 844-7020; E-mail: rmsharkey@gscancer.org.

[3] The abbreviations used are: bsMAb, bispecific antibody or antibodies; CEA, carcinoembryonic antigen; CSAp, colon-specific antigen-p; DOTA, 1,4,7,10-tetraazacyclododecane-*N*, *N′*, *N″*, *N‴*-tetraacetic acid; DTPA, diethylenetriaminepentaacetic; In, indium; Y, yttrium; Re, rhenium; GI, gastrointestinal; h, humanized; HSG, histamine-succinyl-glycine; Tc, technetium; ITLC, instant thin-layer chromatography; PDM, *O*-phenylenedimaleimide; %ID/g, percent injected dose per gram tissue; Lu, lutetium; SE-HPLC, size-exclusion high-pressure liquid chromatography; T:NT, tumor:nontumor ratio; Tscg-Cys, (3-thiosemicarbazonyl)glyoxylcysteinyl.

the antibody. Most bsMAbs have only one binding site for the primary target with the other antibody arm directed to the effector molecule, whereas the streptavidin/avidin-biotin pretargeting systems have typically used a whole IgG with two arms for binding the target, which strengthens target binding. However, Le Doussal *et al.* (9) and Goodwin *et al.* (10) showed that by using a divalent peptide, an affinity enhancement is achieved, which greatly improves the binding of the peptide to the target site compared with a monovalent peptide. Constructing a bsMAb that binds divalently to the tumor antigen can also increase the retention of a bsMAb in the tumor, but care should be taken to minimize the size of such bsMAbs to optimize their clearance kinetics (11). Thus, both the bsMAb and avidin-biotin pretargeting systems are likely to improve tumor imaging and potentially therapy.

Pretargeting with a bsMAb also requires one arm of the antibody to recognize an effector molecule. Most radionuclide targeting systems reported to date have relied on an antibody to a chelate-metal complex, such as antibodies directed to indium-loaded DTPA (12, 13) or antibodies to other chelates (10, 14). Because the antieffector antibody is generally highly selective for the particular chelate-metal complex, new bsMAbs would need to be constructed with the particular effector antibody. This could be avoided if the antibody was not specific to the effector, but instead reacted with another substance. In this way, a variety of effectors could be made so long as they also contained the antibody recognition substance. Janevik-Ivanovska *et al.* (15) described a pretargeting system that used an antibody directed against a histamine derivative, HSG (Fig. 1), as the recognition system on which a variety of effector substances could be prepared. Pretargeting results were reported using a radioiodinated and a rhenium-labeled divalent HSG-containing peptide (15, 16). In this work, we have advanced this system to include peptides suitable for radiolabeling ^{90}Y, ^{111}In, and ^{177}Lu, as well as an alternative peptide for binding technetium and rhenium, thus expanding the applicability of this new approach to cancer therapy with a broader spectrum of radionuclides of current clinical interest. It was also of interest to assess how another antigen associated with colorectal cancer, CSAp, compared with CEA as a target in pretargeting radioimmunotherapy.

MATERIALS AND METHODS

Preparation of bsMAbs. The bispecific F(ab′)$_2$ antibody composed of Fab′ fragments of humanized MN-14 anti-CEA (17), or murine Mu-9 anti-CSAp (18–20) and murine 679 (15) were prepared using PDM as the cross-linker. The F(ab′)$_2$ of each parental antibody was first prepared. For hMN-14 or Mu-9, the F(ab′)$_2$ was reduced with 1 mM of DTT to Fab′-SH, which was diafiltered into a pH 5.3 acetate buffer containing 0.5 mM EDTA (acetate/EDTA buffer) to remove DTT, concentrated to 5–10 mg/ml, and stored at 2–8°C until needed. For 679, the F(ab′)$_2$ was reduced with 1 mM of DTT to Fab′-SH, which was then diluted with 5 volumes of the acetate/EDTA buffer, followed by a rapid addition of 20 mM of PDM (prepared in 90% dimethyl formamide) to a final concentration of 4 mM. After stirring at room temperature for 30 min, the resulting solution (containing 679 Fab′-PDM) was diafiltered into the acetate/EDTA buffer until free PDM was minimized, and concentrated to 5–10 mg/ml. A solution of hMN-14 Fab′-SH or Mu-9 Fab′-SH was then mixed with a solution of 679 Fab′-PDM at a 1:1 ratio based on the amount of Fab′. Adding cysteine to a final concentration of 2 mM quenched the conjugation reaction and the desirable bispecific conjugate (M_r ~ 100,000) was obtained after purification on a Superdex 200-packed column (Amersham, Pharmacia Bio, Piscataway, NJ). The bispecific conjugates were analyzed by SE-HPLC, SDS-PAGE, and isoelectric focusing. For hMN-14 × m679 F(ab′)$_2$, the bispecificity was demonstrated by BIAcore as well as by SE-HPLC. In addition, the affinity of hMN-14 × 679 for HSG was determined by BIAcore analysis using a CM-5 chip derived with a peptide containing a single HSG substituent and a thiol by the disulfide attachment method recommended by the manufacturer (Biacore, Inc., Piscataway, NJ).

IMP 241	DOTA-Phe-Lys(HSG)-D-Tyr-Lys(HSG)-NH$_2$	MH$^+$ 1471
IMP 243	Ac-Lys(HSG)-D-Tyr-Lys(HSG)-Lys(Tscg-Cys)-NH$_2$	MH$^+$ 1340
IMP 245	DOTA-Phe-Lys(HSG)-D-Tyr-Lys(HSG)-Lys(Tscg-Cys)-NH$_2$	MH$^+$ 1832

where TscgC is thiosemicarbazonyl-glyoxyl-cysteinyl-

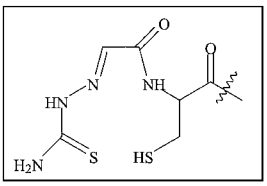

Fig. 1. Chemical structure of HSG, the peptides, and the ^{99m}Tc-binding agent.

For biodistribution studies, the hMN-14 × m679 F(ab′)$_2$ was radioiodinated with ^{125}INa (Perkin-Elmer Life Science, Inc., Boston, MA) by the chloramine-T method (21) and purified using centrifuged size-exclusion columns. Quality assurance testing found <5% unbound radioiodine by ITLC, >90% of the product migrating as a single peak by SE-HPLC (Bio-Sil SE 250; Bio-Rad, Hercules, CA), and >90% of the radiolabeled product shifting to a higher molecular weight with the addition of an excess of CEA (Scripps Laboratories, San Diego, CA). ^{125}I-mMu-9 × m679 bsMAb was tested in a similar manner, using a partially purified extract from GW-39 human colon xenografts as a source of CSAp, which shifted the elution profile of the mMu-9 × 679 bsMAb to the void fraction of the SE-HPLC column.

hMN-14 Fab′-SH was prepared in a similar manner as described previously (22). ^{99m}Tc-pertechnetate (30 mCi) was added directly to the lyophilized hMN-14- Fab′-SH (1.0 mg) and injected i.v. in animals within 30 min (0.05 mg/animal). This product had 3% unbound ^{99m}Tc by ITLC and an immunoreactive fraction of 92%.

Preparation of HSG-containing Peptides. Immunomedics, Inc. synthesized the HSG-containing peptides using a modification to the method that was described previously (15). Fig. 1 shows the structures of the three peptides. The peptides, IMP-243 and IMP-245, both contain the Tscg-Cys ligand and two HSG groups. IMP-243 is designed to be a neutral peptide when complexed with ^{99m}Tc. IMP-245 will also form a neutral ^{99m}Tc-complex, but the peptide is more hydrophilic. The solid phase synthesis of bis hapten Tscg-Cys peptides has been described previously (23). IMP-243 and IMP-245 were formulated into kits, lyophilized, and radiolabeled with ^{99m}Tc-pertechnetate, as described previously (23). ^{99m}Tc-pertechnetate was provided from a local radiopharmacy (Mallinckrodt, Pine Brook, NJ). Immunomedics, Inc. provided the divalent HSG-peptide, IMP 241 used for ^{90}Y, ^{177}Lu, and ^{111}In radiolabeling. This peptide contains a DOTA ligand to facilitate the binding of these radiometals. It was dissolved in 0.5 M ammonium acetate (pH 4.0) to a concentration of 2.2×10^{-3} M.

Radiolabeling of Peptides. $^{90}YCl_3$ was obtained from Perkin-Elmer Life Sciences, Inc., $^{111}InCl_3$ from IsoTex Diagnostics (Friendswood, TX), and ^{177}Lu from the Research Reactor Facility, University of Missouri-Columbia, (Columbia, MO). ^{111}In-IMP 241 was prepared by mixing 3 mCi of $^{111}InCl_3$ in a plastic conical vial with 0.5 M ammonium acetate [(pH 4.0) 3× volume of $^{111}InCl_3$] and 2.3 μl of IMP 241 [2.2×10^{-3} M in 0.5 M ammonium acetate (pH 4.0)]. After centrifugation, the mixture was heated in a boiling water bath for 30 min and cooled. The mixture was centrifuged, and DTPA was added to a final concentration of 3 mM. After 15 min at room temperature, the final volume was raised to 1.0 ml with 0.1 M sodium acetate (pH 6.5). The amount of unbound isotope was determined by reverse-phase HPLC and ITLC developed in saturated sodium chloride solution. Reverse-phase HPLC analyses were performed on a Waters 8 × 100 mm radial Pak cartridge filled with a C-18 Nova-Pak 4-μm stationary phase. The column was eluted at 1.5 ml/min with a linear gradient of 100% A (0.075% trifluoroacetic acid in water) to 55% A and 45% B, where B was 0.075% of trifluoroacetic acid in 75% acetonitrile and 25% water, over 15 min. At 15 min, solvent was switched to 100% B and maintained there for 5 min before reequilibration to initial conditions. Reverse-HPLC analyses showed a single peak at 11.8 min. Analysis of ^{111}In-IMP 241 mixed with excess m679 IgG on a Bio-Sil SE 250 HPLC gel filtration column showed a peak at the retention time of the antibody, indicating binding to the antibody.

IMP-241 was radiolabeled with ^{90}Y by adding to 15 mCi of $^{90}YCl_3$, three times the volume of 0.5 M ammonium acetate (pH 4.0) and 83.2 μl of IMP 241 [1.1×10^{-4} M in 0.5 M ammonium acetate (pH 4.0)], and ascorbic acid to a

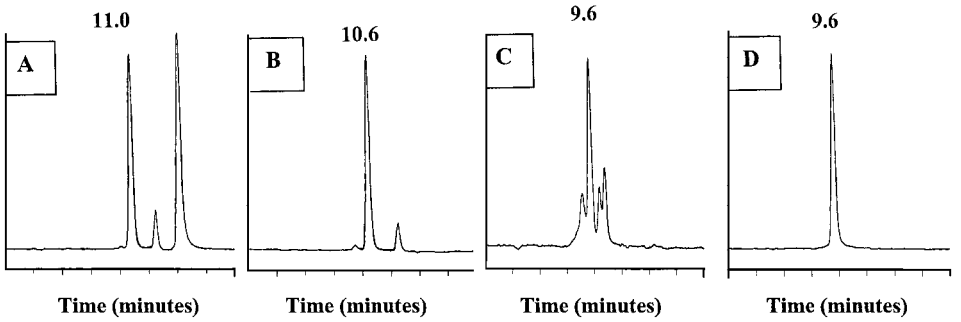

Fig. 2. Preparation of the hMN-14 × m679 bsMAb as monitored by SE-HPLC using an in-line UV detection system. *A*, hMN-14 Fab′-SH treated with *N*-ethylmaleimide to run on HPLC column (peak eluting at latest time is *N*-ethylmaleimide). *B*, m679 Fab-Mal before conjugation. *C*, hMN-14 × m679 bsMAb conjugation mixture before purification. *D*, purified hMN-14 × m679 Fab′ × Fab′ bsMAb.

final concentration of 6.75 mg/ml. The mixture was heated in a boiling water bath for 30 min, and after cooling to room temperature, DTPA was added to a final concentration of 5 mM. Fifteen min later, the final volume was increased to 1.0 ml with 0.1 M sodium acetate (pH 6.5). ITLC strips developed in saturated sodium chloride solution showed <0.2% unbound isotope. Analysis of ^{90}Y-IMP 241 mixed with an excess of m679 IgG by SE-HPLC showed a peak at the retention time of the antibody indicating binding to the antibody.

The stability of the radiolabeled peptides was tested by diluting each of the radiolabeled peptides in mouse serum and incubating the solution at 37°C. Samples were removed at 1, 3, and 24 h and analyzed by reverse-phase HPLC.

***In Vivo* Studies.** GW-39, a CEA-producing human colon cancer cell line (24), was serially propagated in nude mice by mincing 1–2 grams of tumor in sterile physiological saline, passing the minced mixture through a 50-mesh wire screen, and adjusting the saline volume to a final ratio of 10 ml saline/gram tumor. Female NCr nude mice (Charles River Laboratories, Inc., Fredrick, MD, or Taconic, Germantown, NY), ~6 weeks of age were implanted s.c. with 0.2 ml of this suspension. Two to 3 weeks after implantation of tumors, animals were injected with the radiolabeled peptide alone, or, for pretargeting, with the bsMAb followed 1–2 days later with the radiolabeled peptide. For pretargeting, 1.5×10^{-10} moles (15 μg; 6 μCi ^{125}I) of the bsMAb (molecular weight assumed to be M_r 100,000) was injected i.v. (0.1 ml) followed with an i.v. injection (0.1 ml) of ^{111}In-IMP-241 (1.5×10^{-11} moles, 8.8 μCi), ^{177}Lu-IMP-241 (1.5×10^{-11} moles, 5 μCi), or ^{99m}Tc-IMP-243 (1.5×10^{-11}, 25–30 μCi). At the designated times after the peptide injection, animals were anesthetized, bled by cardiac puncture, and then euthanized before necropsy. Tissues were removed, weighed, and counted by γ scintillation using appropriate windows for each radionuclide along with standards prepared from the injected materials. When dual isotope counting was used, appropriate backscatter correction was made. GI tissues (stomach, small intestine, and large intestine) were weighed and counted with their contents. Data are expressed as the %ID/g and the ratio of the percentages in the tumor to the normal tissues (T:NT). All of the values presented in the tables and figures represent the mean and SD of the calculated values with the number of animals used for each study provided therein. Radiation dose estimates are provided according to the methods described earlier (25). This methodology uses S-factors for small spheres comparable with the size of mouse tissues, but only takes into account radiation-absorbed dose from within the source organ. A group of animals given ^{111}In-IMP-241 alone and ^{111}In-IMP-241 24 h after receiving the hMN-14 × m679 bsMAb was also placed in a dose calibrator from the time of the peptide injection at 30-min intervals over 3 h to provide whole-body clearance data.

RESULTS

Radiolabeling of Peptides and Testing of bsMAbs. The DOTA chelation group of IMP-241 was specifically designed for use with ^{111}In and ^{90}Y, but it can also be used with other radiometals, such as ^{177}Lu. The peptide was radiolabeled with each of these radionuclides to specific activities of ~600, 1650, and 300 Ci/mmol, respectively. The lower specific activity for ^{177}Lu was attributed to both the age of the product at the time it was used, and the isotope production run that was not performed in a manner to optimize the specific activity of ^{177}Lu. The specific activity of the ^{99m}Tc-peptides was between 1500 and 1600 Ci/mmol. In each instance radiolabeling conditions were developed to ensure >98% incorporation of the radioactivity in the peptide so that no purification was required. Reverse-phase HPLC indicated that when mixed with fresh mouse serum at 37°C, all of the peptides were stable over 24 h, retaining the original elution profile as seen after their preparation. HPLC analysis of the IMP-243 and 245 on an expanded gradient revealed that the labeled peptide had two peaks (data not shown). The two peaks were probably because of the formation of syn and antitechnetium oxo species.

The kinetic binding of hMN-14 × m679 F(ab′)$_2$ bsMAb to the mono HSG peptide on the chip was evaluated by BIAcore and found to be $K_d = 1.5 \times 10^{-9}$ M. Fig. 2 shows SE-HPLC chromatograms used to monitor the purification of the hMN-14 × m679 bsMAb. The UV profiles of the hMN-14-SH Fab′ and the m679 Fab′-maleimide showed each eluting at 11.0 and 10.6 min, respectively. The unpurified conjugation mixture contained four peaks, including an aggregate, a F(ab′)$_2$, and the individual Fab′ fragments. After purification, a single peak representing the bsMAb F(ab′)$_2$ eluting at 9.6 min was isolated. When each bsMAb F(ab′)$_2$ was radioiodinated, ≥90% of the radiolabeled bsMAb showed binding to CEA or CSAp. This indicates that the ^{125}I-bsMAb is at least 90% immunoreactive or that there is ~10% impurity, hMN-14 F(ab′)$_2$, in bsMAb. Fig. 3 shows the bind-

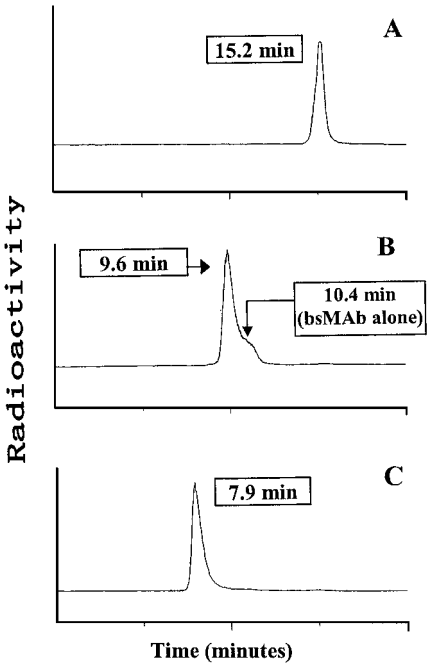

Fig. 3. Binding properties of hMN-14 × m679 bsMAb with ^{111}In-labeled IMP-241 divalent HSG-DOTA peptide. *A*, ^{111}In-IMP-241 alone on SE-HPLC; *B*, ^{111}In-IMP-241 mixed with hMN-14 × 679 bsMAb. Elution time for ^{125}I-bsMAb alone determined in separate run is shown; *C*, ^{111}In-IMP-241 added to a mixture containing hMN-14 × m679 bsMAb with an excess of CEA. Chromatograms show the association of the ^{111}In-IMP-241 with the bsMAb (*B*) and bsMAb/CEA complex (*C*).

Table 1 *Biodistribution of ^{111}In-IMP-241*

Nude mice were injected i.v. with the peptide and necropsied at the times indicated. Values are the means ± SD (n = 4).

Tissue	30 min %ID/g	3 h %ID/g	24 h %ID/g
Tumor	1.42 ± 0.36	0.10 ± 0.03	0.03 ± 0.02
(weight, g)	(0.242 ± 0.245)	(0.179 ± 0.053)	(0.239 ± 0.046)
Liver	0.20 ± 0.03	0.07 ± 0.01	0.06 ± 0.01
Spleen	0.16 ± 0.03	0.04 ± 0.01	0.04 ± 0.01
Kidney	4.07 ± 0.89	2.13 ± 0.21	1.72 ± 0.69
Lungs	0.47 ± 0.07	0.06 ± 0.02	0.02 ± 0.006
Blood	0.39 ± 0.10	<0.01[a]	<0.01[a]
Stomach	0.17 ± 0.15	0.19 ± 0.25	0.01 ± 0.005
Sm. int	0.40 ± 0.20	0.54 ± 0.72	0.02 ± 0.006
Lg. int	0.09 ± 0.01	0.11 ± 0.03	0.03 ± 0.004

[a] Radioactivity concentration below threshold of detection.

Table 2 *Biodistribution of ^{177}Lu-IMP-241*

Nude mice were injected i.v. with the peptide and necropsied at the times indicated. Values are the means ± SD (n = 5).

Tissue	1 h %ID/g	3 h %ID/g	24 h %ID/g
Tumor	0.81 ± 0.20	0.14 ± 0.08	0.03 ± 0.01
(weight, g)	(0.517 ± 0.069)	(0.665 ± 0.261)	(0.538 ± 0.302)
Liver	0.11 ± 0.01	0.08 ± 0.01	0.08 ± 0.01
Spleen	0.11 ± 0.06	0.02 ± 0.01	0.05 ± 0.01
Kidney	3.68 ± 0.57	2.52 ± 0.42	1.76 ± 0.53
Lung	0.20 ± 0.06	0.05 ± 0.01	0.03 ± 0.01
Blood	0.15 ± 0.04	<0.01[a]	<0.01[a]
Stomach	0.09 ± 0.08	0.08 ± 0.12	0.03 ± 0.01
Sm. int	0.29 ± 0.23	0.21 ± 0.32	0.03 ± 0.01
Lg. int	0.05 ± 0.02	0.36 ± 0.45	0.06 ± 0.04

[a] Radioactivity concentration below threshold of detection.

ing of the hMN-14 × m679 bsMAb to ^{111}In-IMP-241 by SE-HPLC. All of the radiolabeled peptide is shifted to an elution time of 9.6 min, with a shoulder on the descending side. The major peak is indicative of two bsMAbs bound for each mol of peptide, whereas the shoulder is the bsMAb bound with a single peptide, because the ^{125}I-bsMAb alone elutes at 10.4 min (data not shown). When CEA is added to the bsMAb followed by the addition of the radiolabeled peptide, the entire amount of radioactivity shifts to the void fraction (7.9 min). Similar results were found with the mMu-9 × m679 bsMAb when using the CSAp preparation (data not shown). These latter studies illustrate that the bsMAb, after binding to antigen, is capable of binding the peptide; however, we appreciate that this is not definitive evidence that these complexes represent divalent binding of the peptide (*i.e.*, 2 moles CEA to 2 moles bsMAb to 1 mol of peptide).

Peptide Biodistribution. For biodistribution purposes, IMP-241 was radiolabeled with the γ-emitting radionuclides ^{111}In or ^{177}Lu rather than ^{90}Y to facilitate the detection of the peptide in tissues, whereas IMP-243 and IMP-245 were radiolabeled with ^{99m}Tc. In tumor-bearing nude mice, the ^{177}Lu- and ^{111}In-IMP-241 had similar distribution and clearance properties (Tables 1 and 2). In both instances, the peptide was cleared so rapidly from blood that within 3 h after its injection, there was insufficient radioactivity in the blood to quantify accurately, but there was sufficient radioactivity in the major organs to permit quantitation. Whole-body readings of animals (n = 3) given 20 μCi of ^{111}In-IMP-241 and individually placed in a dose calibrator at 30-min intervals showed animals had eliminated >75% of the radioactivity within 1 h with none of the animals having detectable levels of radioactivity (*i.e.*, <1 μCi) at 90 min. Collection of total urinary output was not performed. However, a small amount of urine (0.024 ± 0.004 g) was taken from the bladder in three animals necropsied at 1 h, which accounted for 22 ± 17% of the total injected activity. Urine taken from animals necropsied at 3 h had ≤0.1% of total injected activity. In contrast, animals given the hMN-14 bsMAb followed 24 h later by ^{111}In-IMP-241 had 20–30% of the radioactivity remaining in their body at 90 min. Tissue counting data from animals given ^{111}In-IMP-241 alone or in a pretargeting setting showed <1% of the total injected radioactivity in the GI tract suggesting that the primary route of radioactivity elimination from the body in each case was through renal excretion. A percentage of the injected activity lingered in the kidneys over the monitoring period. At an average kidney weight of 0.15 g, there was only ~0.6% of the total ^{111}In-IMP-241 injected activity in the kidney at 0.5–1.0 h after injection. The majority of the radioactivity was excreted in the urine, but there was also a very small fraction that cleared through the GI tract. From 1–3 h, only about 0.6–0.7% of the total injected activity can be accounted for in all of the GI tissues (*i.e.*, stomach, small, and large intestine). By 24 h, only 0.07% of the radioactivity was in all of the GI tissues. Animals given the ^{177}Lu-IMP-241 alone were also necropsied at 48 h, but because there was not enough radioactivity in the kidneys for accurate reporting, the data are not given in the table. However, the ^{177}Lu-IMP-241 in the kidneys had decreased to a level of 0.94 ± 0.2%ID/g, which represented about a 45% decrease compared with the level seen at 24 h.

The tissue distribution of ^{99m}Tc-IMP-243 alone was considerably different from the IMP-241 (Table 3). There was a slower clearance from the blood, a higher uptake in the liver, and a substantial fraction in the GI tract. For example, 1 h after injection, the small intestine contained 24.3 ± 4.75%ID/g of the ^{99m}Tc-IMP-243, and by 3 h, the activity had shifted to the large intestine. By 24 h, the activity was fully cleared from the body. Thus, the radioactivity was not associated with the GI tissues *per se*, but was in the GI contents, as seen with the progression of the radioactivity through the small and large intestines. Another peptide, IMP-245, had a much smaller fraction of the radioactivity in the GI tissues with less liver and renal retention than that seen with ^{99m}Tc-IMP-243. This suggests that the composition of IMP-245 likely favors the direct clearance of the peptide through the kidneys, whereas more of the IMP-243 is processed through the liver and then excreted in the intestine.

Pretargeting Studies. The hMN-14 × m679 F(ab′)$_2$ bsMAb was used to test the pretargeting capabilities of ^{99m}Tc-IMP-243 and

Table 3 *Biodistribution of ^{99m}Tc-IMP-243 and ^{99m}Tc-IMP-245*

Nude mice were injected i.v. with the peptide and necropsied at the times indicated. Values are the means ± SD (n = 5).

	^{99m}Tc-IMP-243			^{99m}Tc-IMP-245	
Tissue	1 h	3 h	24 h	30 min	3 h
Tumor	1.23 ± 0.38	0.44 ± 0.13	0.10 ± 0.02	2.11 ± 0.36	0.29 ± 0.11
(weight, g)	(0.450 ± 0.179)	(0.379 ± 0.168)	(0.439 ± 0.230)	(0.273 ± 0.032)	(0.275 ± 0.085)
Liver	3.29 ± 1.46	1.29 ± 0.95	0.15 ± 0.04	0.63 ± 0.10	0.24 ± 0.02
Spleen	0.45 ± 0.09	0.22 ± 0.03	0.10 ± 0.04	0.46 ± 0.10	0.10 ± 0.01
Kidney	6.57 ± 1.13	4.12 ± 0.86	1.82 ± 0.33	8.63 ± 2.42	2.38 ± 0.21
Lung	1.09 ± 0.16	0.39 ± 0.04	0.10 ± 0.02	1.40 ± 0.32	0.17 ± 0.02
Blood	0.99 ± 0.12	0.43 ± 0.11	0.07 ± 0.01	1.56 ± 0.43	0.19 ± 0.02
Stomach	1.84 ± 0.55	0.68 ± 0.31	0.14 ± 0.06	0.82 ± 0.82	0.35 ± 0.15
Sm. int	24.3 ± 4.75	2.53 ± 0.95	0.08 ± 0.02	1.19 ± 0.70	0.53 ± 0.33
Lg. int	0.63 ± 0.71	40.0 ± 10.4	0.17 ± 0.06	0.25 ± 0.05	1.13 ± 0.20

Table 4 *Pretargeting of ^{99m}Tc-IMP-243 using hMN-14 × m679 F(ab′)$_2$ bsMAb*

	3 h after peptide injection (n = 5)			24 h after peptide injection (n = 4)		
		^{99m}Tc-IMP-243			^{99m}Tc-IMP-243	
Tissue	^{125}I-bsMAb %ID/g	%ID/g	T:NT	^{125}I-bsMAb %ID/g	%ID/g	T:NT
Tumor (weight, g)	4.78 ± 1.11 (0.547 ± 0.265)	12.25 ± 3.32	—	2.24 ± 0.53 (0.390 ± 0.265)	7.36 ± 3.19	—
Liver	1.17 ± 0.19	2.00 ± 0.35	6.2 ± 1.5	0.27 ± 0.08	0.51 ± 0.13	14.4 ± 4.4
Spleen	2.24 ± 0.57	1.55 ± 0.43	8.4 ± 2.9	0.60 ± 0.23	0.48 ± 0.15	15.9 ± 6.3
Kidney	0.81 ± 0.21	4.52 ± 0.79	2.7 ± 0.5	0.20 ± 0.05	2.08 ± 0.38	3.5 ± 1.3
Lungs	1.02 ± 0.29	2.41 ± 0.60	5.3 ± 1.7	0.24 ± 0.04	0.53 ± 0.12	14.1 ± 4.9
Blood	1.48 ± 0.35	5.31 ± 1.32	2.4 ± 0.6	0.41 ± 0.08	1.08 ± 0.29	6.9 ± 2.3
Stomach	7.61 ± 3.33	1.51 ± 0.64	9.5 ± 4.6	0.57 ± 0.26	0.27 ± 0.14	27.8 ± 1.5
Sm. int	0.51 ± 0.15	5.44 ± 2.42	2.4 ± 0.7	0.10 ± 0.03	0.37 ± 0.21	22.2 ± 8.0
Lg. int	1.22 ± 0.10	24.79 ± 2.82	0.5 ± 0.2	0.09 ± 0.04	0.80 ± 0.48	10.4 ± 3.3

Table 5 *Pretargeting of ^{99m}Tc-IMP-245 using hMN-14 × m679 F(ab)$_2$ bsMAb (24-h clearance of the bsMAb)*

	1 h after peptide injection (n = 5)			3 h after peptide injection (n = 5)			24 h after peptide injection (n = 5)		
		^{99m}Tc-IMP-245			^{99m}Tc-IMP-245			^{99m}Tc-IMP-245	
Tissue	^{125}I-bsMAb %ID/g	%ID/g	T:NT	^{125}I-bsMAb %ID/g	%ID/g	T:NT	^{125}I-bsMAb %ID/g	%ID/g	T:NT
Tumor (weight, g)	3.41 ± 1.19 (0.304 ± 0.089)	10.1 ± 4.6	—	3.31 ± 0.81 (0.383 ± 0.052)	14.2 ± 5.27	—	1.5 ± 0.7 (0.335 ± 0.129)	5.0 ± 2.6	—
Liver	0.35 ± 0.14	1.10 ± 0.22	10.1 ± 0.5	0.44 ± 0.11	0.71 ± 0.13	19.7 ± 6.0	0.12 ± 0.04	0.20 ± 0.03	23.4 ± 10.1
Spleen	0.62 ± 0.15	0.66 ± 0.13	16.4 ± 9.7	0.75 ± 0.17	0.41 ± 0.06	33.7 ± 9.6	0.15 ± 0.03	0.13 ± 0.03	43.4 ± 26.5
Kidney	0.33 ± 0.05	4.80 ± 0.98	2.3 ± 1.4	0.28 ± 0.07	2.68 ± 0.50	5.2 ± 1.6	0.08 ± 0.02	0.89 ± 0.13	5.5 ± 2.8
Lungs	0.28 ± 0.06	1.57 ± 0.40	7.3 ± 5.1	0.26 ± 0.05	0.88 ± 0.14	16.0 ± 5.2	0.10 ± 0.01	0.14 ± 0.02	36.1 ± 21.8
Blood	0.47 ± 0.07	4.16 ± 0.98	2.4 ± 0.6	0.44 ± 0.09	2.23 ± 0.39	6.3 ± 1.7	0.14 ± 0.02	0.19 ± 0.02	26.3 ± 13.3
Stomach	0.92 ± 0.35	0.43 ± 0.06	23.5 ± 11.2	1.19 ± 0.83	0.41 ± 0.45	57.1 ± 29.1	0.21 ± 0.05	0.06 ± 0.02	96.9 ± 68.7
Sm. int	0.12 ± 0.03	0.96 ± 0.11	10.5 ± 4.8	0.12 ± 0.05	0.76 ± 0.23	18.7 ± 4.3	0.04 ± 0.01	0.10 ± 0.04	58.7 ± 36.8
Lg. int	0.18 ± 0.06	0.26 ± 0.14	47.8 ± 32.6	0.19 ± 0.08	0.97 ± 0.46	16.1 ± 7.4	0.04 ± 0.01	0.17 ± 0.08	30.2 ± 9.3

^{99m}Tc-IMP-245. The bsMAb was radiolabeled with ^{125}I so that its distribution could be coregistered with either ^{99m}Tc-IMP-243 or IMP-245. The bsMAb was given to animals i.v., and after 24 h, the radiolabeled peptide was given, and the animals were necropsied 3 and 24 h later. In the pretargeting setting, tumor uptake of the ^{99m}Tc-IMP-243 was nearly 28- and 70-times higher than that seen with peptide alone at 3 and 24 h after its injection (Table 4). Tumor uptake was 12.25 ± 3.32%ID/g at 3 h, reducing to 7.36 ± 3.19 by 24 h. The reduction of ^{99m}Tc-IMP-243 in the tumor over this time was not as high as the reduction of the bsMAb in the tumor, which dropped from 4.78 ± 1.11%ID/g to 2.24 ± 0.53%ID/g over this same period. T:NT ratios for ^{99m}Tc-IMP-243 were all >2:1 within 3 h, except for the large intestine, where the peptide had not yet cleared, but this improved nearly 20-fold by 24 h with the elimination of the radioactivity in the stool. Tumor uptake for ^{99m}Tc-IMP-245 was similar to that seen with ^{99m}Tc-IMP-243 (Table 5), but T:NT ratios favored ^{99m}Tc-IMP-245. Because the peptides are administered by time rather than by when the level of bsMAb reaches a predefined level, the more favorable T:NT ratios for the ^{99m}Tc-IMP-245 were most likely related to the higher amount of bsMAb in the blood and tissues in the study where the ^{99m}Tc-IMP-243 was given (*e.g.*, 0.44 ± 0.09%ID/g at 3 h after the ^{99m}Tc-IMP-245 injection *versus* 1.48 ± 0.35%ID/g 3 h after the ^{99m}Tc-IMP-243 injection). However, ^{99m}Tc-IMP-245 pretargeting also had lower GI uptake, even at 1 h, and therefore this peptide has a distinct advantage over ^{99m}Tc-IMP-243. Tumor uptake and T:NT ratios for the pretargeting procedure using ^{99m}Tc-IMP-245 were also better at 3 h than that achieved with ^{99m}Tc-hMN-14 Fab′ (Table 6), suggesting that pretargeting with ^{99m}Tc-IMP-245 should provide better image contrast at an earlier time than that found with a ^{99m}Tc-Fab′ fragment.

Two different targeting systems were used in the evaluation of pretargeting the IMP-241 peptide, one system using a humanized anti-CEA antibody (hMN-14) and the other a murine antibody to CSAp (mMu-9). Each bsMAb was prepared by chemically coupling its Fab′ to the Fab′ of the murine 679 MAb. For biodistribution studies, each bsMAb was radiolabeled with ^{125}I so that its distribution could be assessed together with the IMP-241, which was radiolabeled with ^{111}In. The amount of bsMAb and peptide injected in tumor-bearing nude mice were the same in each pretargeting system, but because the Mu-9 bsMAb took longer to clear from the blood than the hMN-14 bsMAb, the radiolabeled peptide was given at 48 h after the Mu-9 bsMAb, compared with 24 h after the hMN-14 bsMAb. We have described previously the differences in the clearance rates of bsMAb and the importance of selecting an appropriate interval before administering the radiolabeled peptide (23). By using a 24-h delay for the hMN-14 × m679 construct and a 48-h delay for the mMu-9 × m679 construct, the blood levels of each bsMAb were similar, 0.79 ± 0.24%ID/g and 0.55 ± 0.10%ID/g, respectively (Tables 7 and 8). It was not unexpected to find a higher amount of the Mu-9 bsMAb in the tumor (13.1 ± 4.36%ID/g) than the MN-14 bsMAb (2.92 ± 0.41), because earlier studies comparing the targeting of the Mu-9 and anti-CEA antibodies had found Mu-9 to have a higher uptake and a longer retention in the GW-39 xenograft model than was observed with anti-CEA antibodies (20). With a higher amount of Mu-9 bsMAb in the tumor, a higher concentration of the peptide was achieved, reaching a level of 17.8 ± 1.4%ID/g in just 3 h after the peptide injection, compared with 11.3 ± 2.2%ID/g for the peptide in animals pretargeted with the anti-CEA hMN-14 bsMAb. Interestingly,

Table 6 *Biodistribution of ^{99m}Tc-hMN-14 Fab′ in GW-39 tumor-bearing nude mice[a] 3 h after injection*

Tissue	%ID/g	T:NT
Tumor	1.0 ± 0.2	—
Liver	5.2 ± 0.9	0.2 ± 0.02
Spleen	8.1 ± 2.7	0.1 ± 0.02
Kidney	55.9 ± 3.9	0.02 ± 0.001
Lungs	1.5 ± 0.4	0.7 ± 0.1
Blood	1.0 ± 0.1	1.0 ± 0.01

[a] (n = 5).

Table 7 *Pretargeting of ^{111}In-IMP-241 using hMN-14 × m679 F(ab')$_2$ bsMAb (24-h bsMAb clearance)*

Time	Tissue	^{125}I-bsMAb	^{111}In-241	
		%ID/g	%ID/g	T:NT
3 h after ^{111}In-IMP-241 injection (n = 5)	Tumor (0.254 ± 147 g)	2.92 ± 0.41	11.3 ± 2.2	—
	Liver	0.44 ± 0.24	0.53 ± 0.14	22.2 ± 6.3
	Spleen	0.94 ± 0.41	0.42 ± 0.12	27.8 ± 5.9
	Kidney	0.44 ± 0.17	4.61 ± 0.71	2.5 ± 0.5
	Lungs	0.49 ± 0.24	0.83 ± 0.23	14.1 ± 2.8
	Blood	0.79 ± 0.24	1.44 ± 0.33	8.1 ± 2.1
	Stomach	3.18 ± 2.27	0.11 ± 0.02	102.9 ± 15.2
	Sm. intestine	0.27 ± 0.15	0.23 ± 0.08	53.4 ± 14.4
	Lg. intestine	0.35 ± 0.18	0.31 ± 0.07	37.4 ± 9.2
24 h after ^{111}In-IMP-241 injection (n = 4)	Tumor (0.203 ± 0.090 g)	1.80 ± 0.34	6.87 ± 0.84	—
	Liver	0.10 ± 0.03	0.31 ± 0.05	22.3 ± 2.5
	Spleen	0.35 ± 0.20	0.40 ± 0.13	18.5 ± 5.6
	Kidney	0.11 ± 0.02	2.60 ± 0.43	2.7 ± 0.5
	Lungs	0.13 ± 0.02	0.29 ± 0.05	24.0 ± 5.7
	Blood	0.23 ± 0.03	0.43 ± 0.10	16.4 ± 3.3
	Stomach	0.21 ± 0.06	0.06 ± 0.01	116.9 ± 10.2
	Sm. intestine	0.05 ± 0.01	0.10 ± 0.02	67.3 ± 9.6
	Lg. intestine	0.04 ± 0.01	0.11 ± 0.03	66.0 ± 12.2
48 h after ^{111}In-IMP-241 injection (n = 5)	Tumor (0.206 ± 0.073 g)	1.32 ± 0.15	5.47 ± 1.03	—
	Liver	0.06 ± 0.01	0.27 ± 0.05	20.4 ± 4.1
	Spleen	0.24 ± 0.14	0.40 ± 0.05	13.6 ± 2.0
	Kidney	0.07 ± 0.01	1.17 ± 0.21	4.7 ± 0.46
	Lungs	0.07 ± 0.02	0.19 ± 0.04	28.9 ± 6.5
	Blood	0.11 ± 0.02	0.17 ± 0.03	32.0 ± 7.2
	Stomach	0.09 ± 0.03	0.04 ± 0.02	163.2 ± 53.9
	Sm. intestine	0.03 ± 0.01	0.07 ± 0.02	76.8 ± 16.2
	Lg. intestine	0.02 ± 0.01	0.07 ± 0.02	83.0 ± 16.8

the hMN-14 bsMAb localized in the tumor was apparently more efficient at binding the peptide, because the ratio of the %ID/g of the peptide compared with the bsMAb in the tumor was 3.9 for the hMN-14 bsMAb at 3 h, compared with 1.4 for the Mu-9 bsMAb at this same time. This extrapolated to approximately 13–24% of the Mu-9 bsMAb having at least 1 mol of peptide bound, whereas nearly 38–40% of the hMN-14 bsMAb was occupied with at least 1 mol of peptide. This assumes a 1:1 mol ratio of bsMAb to peptide, but because the peptide is divalent and could bind two bsMAbs, these values could actually be doubled if all of the peptide was divalently bound. In each system, the peptide:bsMAb ratio observed at 3 h was maintained over the 48-h observation period, suggesting that the peptide was bound specifically by the bsMAb. However, ^{111}In-IMP-241 was retained by the tumor in the Mu-9 pretargeting system for a longer period of time than the hMN-14 bsMAb system, which corresponded to the extended time that the bsMAb was bound to the tumor. Pretargeting increased tumor accretion of the ^{111}In-IMP-241 nearly 100-fold compared with the peptide alone (refer to Table 1). With pretargeting, T:NT ratios were also significantly improved for all of the tissues as compared with that seen with the ^{111}In-241 peptide alone, regardless of which bsMAb pretargeting system was used. Overall, T:NT ratios for the ^{111}In-IMP-241 were significantly higher in the Mu-9 bsMAb system, especially over time.

Regardless of whether IMP-241 was radiolabeled with ^{177}Lu or

Table 8 *Pretargeting of ^{111}In-IMP-241 using mMu-9 × m679 F(ab')$_2$ bsMAb (48-h bsMAb clearance)*

Time	Tissue	^{125}I-bsMAb	^{111}In-241	
		%ID/g	%ID/g	T:NT
3 h after ^{111}In-IMP-241 injection	Tumor (0.164 ± 0.064 g)	13.1 ± 4.36	17.8 ± 1.4	—
	Liver	0.19 ± 0.03	0.56 ± 0.08	32.0 ± 3.0
	Spleen	0.28 ± 0.12	0.46 ± 0.13	41.2 ± 10.6
	Kidney	0.32 ± 0.04	3.63 ± 0.34	4.9 ± 0.5
	Lungs	0.31 ± 0.05	0.92 ± 0.21	20.0 ± 2.9
	Blood	0.55 ± 0.10	1.93 ± 0.63	9.7 ± 2.0
	Stomach	0.75 ± 0.21	0.15 ± 0.07	130.2 ± 41.0
	Sm. intestine	0.11 ± 0.02	0.28 ± 0.12	70.5 ± 20.4
	Lg. intestine	0.10 ± 0.02	0.20 ± 0.07	98.1 ± 27.9
24 h after ^{111}In-IMP-241 injection	Tumor (0.214 ± 0.040 g)	12.4 ± 4.2	17.5 ± 4.1	—
	Liver	0.10 ± 0.02	0.44 ± 0.10	39.8 ± 6.5
	Spleen	0.15 ± 0.05	0.35 ± 0.08	50.3 ± 7.1
	Kidney	0.15 ± 0.03	2.28 ± 0.35	7.7 ± 1.9
	Lungs	0.12 ± 0.02	0.31 ± 0.05	56.0 ± 6.0
	Blood	0.22 ± 0.05	0.38 ± 0.12	47.6 ± 11.2
	Stomach	0.17 ± 0.04	0.05 ± 0.01	377.6 ± 101.8
	Sm. intestine	0.05 ± 0.01	0.09 ± 0.02	195.7 ± 49.7
	Lg. intestine	0.03 ± 0.01	0.08 ± 0.02	235.8 ± 58.4
48 h after ^{111}In-IMP-241 injection	Tumor (0.213 ± 0.064 g)	11.2 ± 5.5	12.7 ± 4.8	—
	Liver	0.06 ± 0.01	0.29 ± 0.06	44.6 ± 16.2
	Spleen	0.06 ± 0.01	0.25 ± 0.05	50.6 ± 14.1
	Kidney	0.06 ± 0.01	0.99 ± 0.35	12.9 ± 2.6
	Lungs	0.05 ± 0.01	0.14 ± 0.01	90.8 ± 32.3
	Blood	0.07 ± 0.01	0.10 ± 0.02	127.8 ± 41.7
	Stomach	0.10 ± 0.04	0.04 ± 0.01	338 ± 148.5
	Sm. intestine	0.02 ± 0.00	0.07 ± 0.01	189.9 ± 71.1
	Lg. intestine	0.02 ± 0.01	0.07 ± 0.02	168.0 ± 40.9

^{111}In, the pretargeting results were the same. As seen in Table 9, using the hMN-14 bsMAb pretargeting system, the %ID/g of the ^{177}Lu-IMP-241 was identical to that seen with ^{111}In-IMP-241. Because the distribution of ^{111}In-IMP-241 mimicked ^{177}Lu-IMP-241, and because ^{111}In has also been used as a surrogate for predicting ^{90}Y-distribution, an extended biodistribution study was performed using the ^{111}In-IMP-241 and the mMu-9 × m679 F(ab′)$_2$ bsMAb. As shown in Fig. 4, as a consequence of extended retention of the Mu-9 antibody in the tumor (biological half-life = 94 h), there was also an extended retention of the radiolabeled peptide in the tumor (biological half-life = 127 h). Using these data, radiation dose estimates were modeled for ^{90}Y and ^{177}Lu (Table 10). ^{90}Y, because of its higher β-radiation energy (2.27 meV$_{max}$), delivers a higher radiation dose to the tumor than ^{177}Lu (495 keV$_{max}$) on a per-mCi basis. However, to allow for a better comparison, the radiation doses were normalized to reflect an identical radiation to a dose-limiting organ. In this case, 1,500 cGy to the kidneys was selected as a dosage that should be tolerated but could result in similar toxicities. When the absorbed doses to the tissues were normalized, the data suggest that ^{177}Lu-IMP-241 would potentially deliver the same dose to the tumor as ^{90}Y-IMP-241. If the kidneys were able to tolerate 1,500 cGy, then the tumor would receive nearly 12,000 cGy, a radiation dose that should be lethal to most solid tumors.

DISCUSSION

bsMAbs can be prepared against any target antigen, but the primary limitation has been the need to have the other arm of the bsMAb highly specific for a particular carrier molecule. This specificity is necessary so that the bsMAb will bind selectively and with high affinity to that carrier. With radionuclides, different carriers are often required to optimize the stability of the carrier-radionuclide conjugate. For example, the anti-DTPA antibody, 734, used by Le Doussal *et al.* (13) and by our group (23) is highly specific for In-loaded DTPA, and as such could be used in conjunction with a number of antitumor antibodies and an appropriate ^{111}In-labeled carrier. By simply having a tyrosine residue in the divalent-DTPA peptide so that the peptide could be radioiodinated, the utility of a bsMAb pretargeting system using MAb 734 was expanded (26). By loading the DTPA with In for high-affinity 734 binding and then radioiodinating the peptide, this system has been used for therapy with ^{131}I attached to the carrier molecule (27, 28). We have additionally expanded on this system by developing a divalent DTPA peptide with a ligand suitable for technetium and rhenium binding (23). However, this system could not be used with other radiometals of therapeutic interest, such as ^{90}Y, because MAb 734 was more specific for In-loaded DTPA than Y-loaded DTPA, and ^{90}Y was not very stable in the DTPA. Although divalent DTPA peptides could be prepared with other chelating agents (*e.g.*, DOTA), the DTPA component of the peptide would inevitably bind other metals, but less stably, which would likely result in their dissociation from the peptide and unwanted uptake in normal tissues, such as the bone. A more logical approach to making a bsMAb system that potentially could be used in a wider array of applications would be to have an antibody directed against a carrier that was not directly involved in the binding of the radionuclide.

Goodwin *et al.* (29) suggested the need for developing a system with greater flexibility for use in imaging and therapy applications. For this purpose, the antibody must be directed against a unique substance that is not found in the body to avoid misdirecting the bsMAb to unintended targets, and the substance should be small and amenable to coupling so that it could be used in a variety of compounds. These criteria can be found in a system first described by Le Doussal *et al.* (9), but more thoroughly tested by Janevik-Ivanovska *et al.* (15), and this system relied on an antibody directed against a derivative of histamine, HSG, for recognition of the carrier (30). The antibody, designated 679, was very specific for HSG, having nearly a four-log lower affinity for histamine. Janevik-Ivanovska *et al.* (15) synthesized several HSG-containing peptides suitable for radiolabeling with iodine by including a tyrosine residue in the peptide structure. D-Tyrosine was used, because previous studies had shown that this greatly stabilized another peptide of similar composition (26). Studies that examined the ^{125}I-HSG-peptide isolated from mouse serum confirmed its stability. They also found that the positioning and length of peptide was important in preserving the highest level of affinity to the 679 MAb. The peptides IMP-241, IMP-243, and IMP-245 were prepared so as to retain the optimal HSG arrangement in accordance with the findings of these investigators. Pretargeting studies in nude mice bearing human colon tumor xenografts with the F6 anti-CEA antibody × 679 F(ab′)$_2$ bsMAb and a ^{125}I-labeled divalent HSG-peptide showed rapid tumor accretion of the peptide, with highly favorable

Table 9 *Comparison of ^{111}Lu-IMP-241 and ^{111}In-IMP-241 pretargeting using the hMN-14 × m679 F(ab′)$_2$ bsMAb (24 h bsMAb clearance)*

Time	Tissue	Percent injected dose per gram	
		^{177}Lu-IMP-241	^{111}In-IMP-241
3 hours after radiolabeled peptide injection	Tumor (weight, g)	9.71 ± 2.49 (0.747 ± 0.243)	8.76 ± 2.31 (0.536 ± 0.114)
	Liver	0.46 ± 0.08	0.57 ± 0.24
	Spleen	0.36 ± 0.04	0.54 ± 0.30
	Kidney	3.61 ± 0.43	3.00 ± 0.87
	Lungs	0.64 ± 0.12	0.81 ± 0.33
	Blood	1.48 ± 0.19	1.87 ± 0.97
24 hour after radiolabeled peptide injection	Tumor (weight, g)	2.59 ± 0.30 (0.723 ± 0.138)	2.54 ± 1.04 (0.405 ± 0.105)
	Liver	0.17 ± 0.04	0.19 ± 0.07
	Spleen	0.29 ± 0.07	0.28 ± 0.10
	Kidney	0.18 ± 0.03	0.25 ± 0.14
	Lungs	0.17 ± 0.02	0.24 ± 0.07
	Blood	0.36 ± 0.05	0.54 ± 0.20

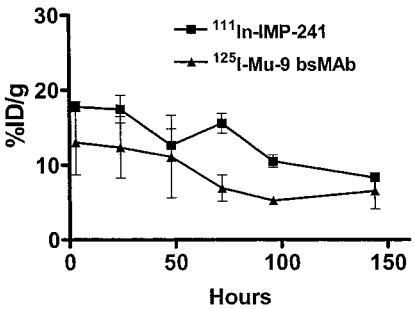

Hours	Peptide/bsMAb Ratio
3	0.148 ± 0.044
24	0.150 ± 0.054
48	0.121 ± 0.036
72	0.238 ± 0.082
96	0.199 ± 0.021
144	0.141 ± 0.049

Fig. 4. Clearance of ^{125}I-mMu-9 × m679 F(ab′)$_2$ bsMAb and ^{111}In-IMP-241 in GW-39 tumor-bearing nude mice. Mice were injected i.v. with the radiolabeled bsMAb, and 48 h later the radiolabeled peptide was given i.v. Values represent the mean of the percent injected dose per gram (n = 5 for each time interval); *bars*, ±SD. The table shows the ratio of the moles of peptide per gram tumor compared with that of the bsMAb.

Table 10 *Dosimetry for ^{90}Y- or ^{177}Lu-labeled IMP-241 using the mMu-9 × m679 F(ab′)$_2$ bsMAb*

Tissue	^{90}Y-IMP-241		^{177}Lu-IMP-241	
	cGy/mCi	cGy (normalized)[a]	cGy/mCi	cGy (normalized)[a]
Tumor	14,366	12,578	5580	13,721
Blood	416	364	124	305
Liver	551	482	161	394
Lungs	277	242	94	231
Kidneys	1713	1500	610	1500

[a] Radiation absorbed doses are normalized to 1500 cGy to the kidneys.

T:NT ratios within 3 h after its injection (15). More recently, Gestin *et al.* (31) described a divalent HSG-peptide for both radioiodination and technetium/rhenium radiolabeling. This peptide, which included an *S*-acetylthioacetyl residue for ^{188}Re binding, proved to be unstable with respect to its ability to bind ^{188}Re and, therefore, dosimetry estimates predicted a higher therapeutic ratio for the ^{131}I-peptide compared with the ^{188}Re peptide. We did not test IMP-243 and IMP-245 with rhenium, but based on previous data using another peptide with the same Tscg-Cys binding group (23), these peptides might provide a greater stability for rhenium. As shown in Table 11, all three of the peptides studied herein had favorable properties for pretargeting, with the only possible exception being the early hepatic uptake and subsequent clearance of ^{99m}Tc-IMP-243 through the GI tract, which could interfere with early imaging of the abdomen and pelvis.

Our group has focused initially on the development of this system in conjunction with DOTA, a chelate known for its high affinity for binding ^{90}Y and even ^{177}Lu. Both of these radionuclides have been conjugated directly to antibodies for cancer therapy (32, 33), and ^{90}Y-biotin also has been used in combination with streptavidin pretargeting (34). The high β-energy (2.27 meV_{max}, 0.93 meV_{ave}) of ^{90}Y gives this radionuclide an average range of ~5 mm in tissue, ideal for treating larger tumors, whereas ^{177}Lu has a moderate β-energy (495 keV_{max}, 133 keV_{ave}) and a range of ~0.6 mm in tissue, being more optimal for smaller, even micrometastatic tumors. The pretargeting approach seems to be ideally suited for both of these radionuclides, because the nontargeted, peptide-bound radionuclide is rapidly removed from the body, yielding higher concentrations in the tumor than in normal tissues within just 3 h after the injection of the radiolabeled peptide. The use of a divalent HSG-peptide creates an affinity enhancement system that is responsible in part for the high level of peptide binding in the tumor. These studies also showed that the binding characteristics of the primary targeting antibody were important for optimizing tumor localization and retention of the radiolabeled peptide. This is particularly important for isotopes with a long physical half-life, such as ^{177}Lu (161 h) or ^{131}I (193 h), because it means the tumor will continue to be irradiated throughout its decay period, whereas the normal tissues are spared of this exposure. In this regard, the Mu-9 (CSAp) bsMAb pretargeting system is expected to be better suited for longer-lived isotopes, because of its longer tumor retention than the hMN-14 (CEA) system.

Thus, pretargeting is not only ideally suited for isotopes of short physical half-life, because favorable T:NT ratios are developed so rapidly, but potentially also for those with a longer physical decay because the radioactivity is held in the tumor for several days. It is not entirely clear what, if any, limitations might be placed on the physical half-life of a radionuclide for therapeutic applications. Isotopes with a very short half-life, such as bismuth-213 (with a half-life of only 45 min), would be expected to be too short for even pretargeting to provide an acceptable tumor localization advantage, particularly when the vast majority of the injected activity is excreted through the kidneys in less than 1 h, which might make it difficult to deliver a higher dose to the tumor compared with the kidney. However, radiation dose estimates in another pretargeting system using a hMN-14 × anti-DTPA antibody and a ^{188}Re-labeled peptide suggested that ^{188}Re, with a half-life of ~18 h, may be suitable for systemic pretargeting therapy (23). Studies performed herein suggest the possibility of using ^{90}Y- as well as ^{188}Re-labeled peptides. Because the βemissions of these two radionuclides are very similar, but they have different physical half-lives, comparative efficacy studies at equitoxic doses would be useful in defining certain properties of a suitable radionuclide to be used in pretargeting. Preclinical studies using an anti-CEA bsMAb and a ^{131}I-labeled peptide have already shown therapeutic responses, indicating that ^{131}I, with a physical half-life of ~8 days, is a suitable candidate (28). Indeed, if the targeted peptide were retained in the tumor for extended periods, and with the rapid development of T:NT ratios exceeding 2:1, radionuclides with long physical half-lives could be highly advantageous, especially if there was progressive renal clearance. Pilot clinical studies using an hMN-14 × anti-DTPA bsMAb and a ^{131}I-labeled peptide are being pursued currently to assess the optimal pretargeting conditions. Although not yet fully optimized, the early results from this trial have shown that the ^{131}I peptide is retained in the tumor with a terminal half-life in the tumor of ~4 days, and with tumor doses averaging 19.2 cGy/mCi *versus* renal doses of 2.7 cGy/mCi (35).

The preclinical studies described herein suggest that ^{177}Lu, with a half-life of 161 h, might also be suitable for systemic pretargeting therapy. With the potential to use isotopes with different β energies, therapeutic benefits might be possible when treating micrometastatic disease, as well as tumors of more substantial size with this single targeting system. Although much of our effort thus far has focused on the use of this system with radionuclides, it should be possible to design other di-HSG-containing peptides with other substances of therapeutic interest. This suggests the possibility of combining different modalities of treatment with a single targeting system.

Although isotopes with half lives <1 h might not be ideally suited for therapy, T:NT ratios for this pretargeting approach using ^{99m}Tc-labeled peptides were sufficiently favorable even at 1 h, such that for imaging applications, isotopes with a short physical half-life could be considered. Studies comparing the IMP-243 to the IMP-245 peptide, each containing the Tscg-Cys ligand for binding technetium and rhenium, suggested that the structure of the peptide was important for determining the biodistribution of the peptide. Studies with ^{99m}Tc-IMP-243 alone showed substantially higher amounts of radioactivity in the liver at 1 h compared with the ^{99m}Tc-IMP-245 with evidence of GI excretion (Table 3), whereas there was no appreciable GI transit of ^{99m}Tc-IMP-245, suggesting that urinary excretion was the primary route of clearance for this peptide. The clearance behavior of these two peptides may be related to their different lipophilic nature, because, as reported by Trejtnar *et al.* (36), the route of excretion for ^{99m}Tc-labeled peptides through the hepatic/biliary/GI tract or by the urinary tract is affected by this property. Although pretargeting using ^{99m}Tc-IMP-243 might still be useful for imaging because T:NT ratios exceeded 2:1 for all of the critical organs at 3 h, the transit of ~25% of the total radioactivity through the GI tract is considered undesirable. In contrast, the lack of GI uptake by ^{99m}Tc-IMP-245 and with T:NT in a pretargeting system exceeding 2:1 1 h after the peptide injection, this is a more favorable targeting system for imaging. Indeed, localization with this pretargeting approach using the anti-CEA bsMAb substantially exceeded the targeting ratios seen with a

Table 11 *Properties of the IMP-peptides*

Peptide	Used with	Properties
IMP-241	^{111}In, ^{90}Y, ^{177}Lu (any DOTA-binding metal)	Can be radiolabeled to high specific activity Rapid clearance from blood No hepatic or GI uptake Low retention and gradual clearance from kidney
IMP-243	^{99m}Tc/^{188}Re/^{186}Re	Can be radiolabeled to high specific activity (^{99m}Tc-tested) Rapid clearance from blood Early uptake in liver with subsequent clearance through GI tract Low retention and gradual clearance from kidney
IMP-245	^{99m}Tc/^{188}Re/^{186}Re ^{111}In/^{90}Y/ ^{177}Lu	Can be radiolabeled to high specific activity Radiolabeling with ^{111}In/^{90}Y/^{177}Lu may be possible Rapid clearance from blood No hepatic or GI uptake (^{99m}Tc-peptide) Low retention and gradual clearance from kidney

directly radiolabeled ^{99m}Tc-hMN-14 Fab′. Because a ^{99m}Tc-labeled anti-CEA Fab′ has been used successfully for imaging patients within 2 h (37, 38), the contrast ratios obtained with the pretargeting approach suggest that image contrast could be improved using ^{99m}Tc-IMP-245, with the possibility for even earlier tumor imaging. If high contrast ratios could be achieved within 2 h clinically, then peptides with positron-emitting isotopes, many of which have physical half-lives of 1–2 h, could conceivably be used. Indeed, Klivényi *et al.* (39) and Schuhmacher *et al.* (40) already have shown the feasibility of using a bsMAb pretargeting approach with gallium-68-chelators.

In the tumor model used for these studies, the Mu-9 anti-CSAp bsMAb had a higher percentage of uptake and longer tumor retention than the hMN-14 anti-CEA bsMAb. We are uncertain why the Mu-9 antibody shows a preference for binding to colorectal cancer xenografts over anti-CEA antibodies (20). Indeed, *in vitro*, Mu-9 binds very weakly to colon cancer cell lines compared with anti-CEA antibodies,[4] suggesting that the antigen might not be well expressed on the cell surface. Immunohistology reveals very intense staining of the cytoplasm, and in well-differentiated tumors the apical borders of the malignant crypts are stained heavily. However, Mu-9 consistently has shown higher binding *in vivo* to both GW-39 (20) and LS174T human colonic cancer xenografts than anti-CEA antibodies, additionally suggesting that the antigen may be shed by the cells and become trapped within the mucin surrounding the cells, thereby making it accessible for antibody binding. Irrespective of the reason for the binding preference of Mu-9, this improved binding impacted positively on the subsequent localization of the peptide. It is also worth noting that the CSAp epitope recognized by Mu-9 does not appear to be detected in the blood of cancer patients (41), suggesting that Mu-9 may be even more optimal than CEA as a target for the bsMAb in pretargeting methods, because binding of the bsMAb to circulating antigen would be precluded. Interestingly, the hMN-14 (CEA) bsMAb was apparently more efficient at binding the peptide in the tumor than the Mu-9 (CSAp) bsMAb, with nearly 35% of the hMN-14 bsMAb binding to the peptide, whereas only 18% of the Mu-9 bsMAb bound to the peptide. The specific mechanism to explain this finding is as yet not known. Although both bsMAbs were prepared identically to orient the two Fab′ fragments in a similar manner, it is still possible that there might be differential binding of the peptide, especially after the bsMAb is bound to antigen. Direct measurements of the binding affinity of the HSG binding portion of the Mu-9 bsMAb by BIAcore was not undertaken, because the antigen (CSAp) has not been isolated so that an appropriate chip could be made. Thus, these results could reflect different affinities for the peptide-binding portion of the bsMAb when bound to antigen, but there may also be a different accessibility and orientation of the bsMAb within the tumor that could have affected peptide binding. It is also important to remember that these results may merely reflect differences in the portion of the peptide that is divalently bound to the bsMAb.

In conclusion, we have demonstrated that the HSG targeting system offers considerable flexibility in the choice of substances that can be used in this pretargeting methodology. The flexibility of this targeting system for a variety of radionuclides has been shown herein for ^{111}In, ^{99m}Tc, ^{90}Y, and ^{177}Lu, whereas others have used different HSG-peptides suitable for ^{188}Re/^{99m}Tc and ^{131}I radiolabeling (26, 31). Preliminary studies with an engineered recombinant anti-CEA × 679 bsMAb have confirmed the potential to create new proteins with enhanced clearance properties, but with similar retention in the tumor as the chemically conjugated bsMAb (42). Thus, because different targeting moieties (isotopes, drugs, and contrast agents) conceivably could be attached to the HSG carrier for use with diverse bsMAbs that have at least one binding site for HSG, this system may have diverse applications for both disease imaging and therapy by designing appropriate HSG-carrier systems.

[4] R.M. Sharkey and H. Karacay, unpublished observations.

ACKNOWLEDGMENTS

We thank Dr. Michele Losman, Dr. Lee Zhang, Gaik Lin Ong, and Guy Newsome for their assistance in the production of bsMAbs, Heidi Richel with the animal studies, Phil Andrew in radiolabeling, and Dr. David V. Gold for providing CSAp.

REFERENCES

1. Chang, C-H., Sharkey, R. M., Rossi, E. A., Karacay, H. McBride, W., Hansen, H. J., Chatal, J-F., Barbet, J., and Goldenberg, D. M. Molecular advances in pretargeting radioimmunotherapy with bispecific antibodies. Mol. Cancer Ther., *1:* 553–563, 2002.
2. Goodwin, D. A., and Meares, C. F. Pretargeted peptide imaging and therapy. Cancer Biother. Radiopharm., *14:* 145–152, 1999.
3. Yuan, F., Baxter, L. T., and Jain, R. K. Pharmacokinetic analysis of two-step approaches using bifunctional and enzyme-conjugated antibodies. Cancer Res., *51:* 3119–3130, 1991.
4. Hnatowich, D. J., Virzi, F., and Rusckowski, M. Investigations of avidin and biotin for imaging applications. J. Nucl. Med, *28:* 1294–1302, 1987.
5. Paganelli, G., Riva, P., Deleide, G., Clivio, A., Chiolerio, F., Scassellati, G. A., Malcovati, M., and Siccardi, A. G. *In vivo* labeling of biotinylated monoclonal antibodies by radioactive avidin: a strategy to increase tumor radiolocalization. Int. J. Cancer, *2*(Suppl.)*:* 121–125, 1988.
6. Axworthy, D. B., Reno, J. M., Hylarides, M. D., Mallett, R. W., Theodore, L. J., Gustavson, L. M., Su, F., Hobson, L. J., Beaumier, P. L., and Fritzberg, A. R. Cure of human carcinoma xenografts by a single dose of pretargeted yttrium-90 with negligible toxicity. Proc. Natl. Acad. Sci. USA, *97:* 1802–1807, 2000.
7. Reardan, D. T., Meares, C. F., Goodwin, D. A., McTigue, M., David, G. S., Stone, M. R., Leung, J. P., Bartholomew, R. M., and Frincke, J. M. Antibodies to metal chelates. Nature (Lond.), *316:* 265–268, 1985.
8. Goodwin, D. A., Meares, C. F., McCall, M. J., McTigue, M., and Chaovapong, W. Pre-targeted immunoscintigraphy of murine tumor with indium-111-labeled bifunctional haptens. J. Nucl. Med., *29:* 226–234, 1988.
9. Le Doussal, J-M., Martin, M., Gautherot, E., Delaage, M., and Barbet, J. *In vitro* and *in vivo* targeting of radiolabeled monovalent and divalent haptens with dual specificity monoclonal antibody conjugates: Enhanced divalent hapten affinity for cell bound antibody conjugates. J. Nucl. Med., *30:* 1358–1366, 1989.
10. Goodwin, D. A., Meares, C. F., McTigue, M., Chaovapong, W., Diamanti, C. I., Ransone, C. H., and McCall, M. J. Pretargeted immunoscintigraphy: effect of hapten valency on murine tumor uptake. J. Nucl. Med., *33:* 2006–2013, 1992.
11. Karacay, H., Sharkey, R. M., McBride, W. J., Griffiths, G. L., Qu, Z., Chang, K., Hansen, H. J., and Goldenberg, D. M. Pretargeting for cancer radioimmunotherapy with bispecific antibodies: role of the bispecific antibody's valency for the tumor target antigen. Bioconj. Chem., *13:* 1054–1070, 2002.
12. Boerman, O. C., Kranenborg, M. H. G. C., Oosterwijk, E., Griffiths, G. L., McBride, W. J., Oyen, W. J., de Weijert, M., Oosterwijk, J., Hansen, H. J., and Corstens, F. H. M. Pretargeting of renal cell carcinoma: Improved tumor targeting with a bivalent chelate. Cancer Res., *59:* 4400–4405, 1999.
13. Le Doussal, J-M., Gruaz-Guyon, A., Martin, M., Gautherot, E., Delaage, M., and Barbet, J. Targeting of indium 111-labeled bivalent hapten to human melanoma mediated by bispecific monoclonal antibody conjugates: imaging of tumors hosted in nude mice. Cancer Res., *50:* 3445–3452, 1990.
14. Feng, X., Pak, R. H., Kroger, L. A., Moran, J. K., DeNardo, D. G., Meares, C. F., DeNardo, G. L., and DeNardo, S. J. New anti-Cu-TETA and anti-Y-DOTA monoclonal antibodies for potential use in the pre-targeted delivery of radiopharmaceuticals to tumor. Hybridoma, *17:* 125–132, 1998.
15. Janevik-Ivanovska, E., Gautherot, E., Hillairet deBoisferon, M., Cohen, M., Milhaud, G., Tartar, A., Rostene, W., Barbet, J., and Gruaz-Guyon, A. Bivalent hapten-bearing peptides designed for ioidine-131 pretargeted radioimmunotherapy. Bioconj. Chem., *8:* 526–533, 1997.
16. Hosono, M., Hosono, M. N., Kraeber-Bodéré, F., Devys, A., Thédrez, P., Faivre-Chauvet, A., Gautherot, E., Barbet, J., and Chatal. J-F. Two-step targeting and dosimetry for small cell lung cancer xenograft with anti-NCAM/antihistamine bispecific antibody and radioiodinated bivalent hapten. J. Nucl. Med., *40:* 1216–1221, 1999.
17. Sharkey, R. M., Juweid, M., Shevitz, J., Behr, T., Dunn, R., Swayne, L. C., Wong, G. Y., Blumenthal, R. D., Griffiths, G. L., Siegel, J. A., Leung, S., Hansen, H. J., and Goldenberg, D. M. Evaluation of a complementarity-determining region-grafted (humanized) anti-carcinoembryonic antigen monoclonal antibody in preclinical and clinical studies. Cancer Res., *55*: 5935s–5945s, 1995.
18. Nocera, M. A., Shochat, D., Primus, F. J., Krupey, J., Jespersen, D., and Goldenberg, D. M. Representation of epitopes on colon-specific antigen-p (CSAp) defined by monoclonal antibodies. J. Natl. Cancer Inst., *79:* 943–948, 1987.
19. Gold, D. V., Nocera, M. A., Stephens, R., and Goldenberg, D. M. Murine monoclonal antibodies to colon-specific antigen-p (CSAp). Cancer Res., *50:* 6405–6409, 1990.

20. Sharkey, R. M., Gold, D. V., Aninipot, R., Vagg, R., Ballance, C., Newman, E., Ostella, F., Hansen, H. J., and Goldenberg, D. M. Comparison of tumor targeting in nude mice murine monoclonal antibodies directed against different human colorectal cancer antigens. Cancer Res., *50:* 828s–834s, 1990.
21. Greenwood, F. C., and Hunter, W. M. The preparation of I-131 labeled human growth hormone of high specific radioactivity. Biochem. J., *89:* 114–123, 1963.
22. Griffiths, G. L., Goldenberg, D. M., Diril, H., and Hansen, H. J. Technetium-99m, rhenium-186 and rhenium-188 direct-labeled antibodies. Cancer (Phila.), *73*(Suppl.)*:* 761–768, 1994.
23. Karacay, H., McBride, W. J., Griffiths, G. L., Sharkey, R. M., Barbet, J., Hansen, H. J., and Goldenberg, D. M. Experimental pretargeting studies of cancer with a humanized anti-CEA x murine anti-[In-DTPA] bispecific antibody construct and a ^{99m}Tc-/^{188}Re-labeled peptide. Bioconjug. Chem., *11:* 842–854, 2000.
24. Goldenberg, D. M., and Hansen, H. J. Carcinoembryonic antigen present in human colonic neoplasms serially propagated in hamsters. Science (Wash. DC), *175:* 1117–1118, 1972.
25. Sharkey, R. M., Motta-Hennessy, C., Pawlyk, D., Siegel, J. A., and Goldenberg, D. M. Biodistribution and radiation dose estimates for yttrium- and iodine-labeled monoclonal antibody IgG and fragments in nude mice bearing human colonic tumor xenografts. Cancer Res., *50:* 2330–2336, 1990.
26. Le Doussal, J-M., Barbet, J., and Delaage. Bispecific-antibody-mediated targeting of radiolabeled bivalent haptens: Theoretical, experimental, and clinical results. Int. J. Cancer, *7*(Suppl.)*:* 58–62, 1992.
27. Gautherot, E., Le Doussal, J-M., Bouhou, J., Manetti, C., Martin, M., Rouvier, E., and Barbet, J. Delivery of therapeutic doses of radioiodine using bispecific antibody-targeted bivalent haptens. J. Nucl. Med., *39:* 1937–1943, 1998.
28. Gautherot, E., Rouvier, E., Daniel, L., Loucif, E., Bouhou, Manetti, C., Martin, M., J., Le Doussal, J-M., and Barbet, J. Pretargeted radioimmunotherapy of human colorectal xenografts with bispecific antibody and ^{131}I-labeled bivalent hapten. J. Nucl. Med., *41:* 480–487, 2000.
29. Goodwin, D. A., Chaovapong, W., Meares, C. F., and McCall, M. J. New monoclonal antibodies for targeting radiopharmaceuticals. J. Nucl. Med., *28:* 561, 1987.
30. Morel, A., Darmon, M., and Delaage, M. Recognition of imidazole and histamine derivatives by monoclonal antibodies. Mol. Immunol., *27:* 995–1000, 1990.
31. Gestin, J. F., Loussouarn, A., Bardiès, Gautherot. E., Gruaz-Guyon, A., Saï-Maurel, C., Barbet, J., Curet, C., Chatal, J. F., and Faivre-Chauvet, A. Two-step targeting of xenografted colon carcinoma using a bispecific antibody and ^{188}Re-labeled bivalent hapten: Biodistribution and dosimetry studies. J. Nucl. Med., *42:* 146–153, 2001.
32. Wiseman, G. A., White, C. A., Sparks, R. B., Erwin, W. D., Podoloff, D. A., Lamonica, D., Bartlett, N. L., Parker, J. A., Dunn, W. L., Spies, S. M., Belanger, R., Witzig, T. E., and Leigh, B. R. Biodistribution and dosimetry results from a phase III prospectively randomized controlled trial of Zevalin radioimmunotherapy for low-grade, follicular, or transformed B-cell non-Hodgkin's lymphoma. Crit. Rev. Oncol. Hematol., *39:* 181–194, 2001.
33. Meredith, R. F., Alvarez, R. D., Partridge, E. E., Khazaeli, M. B., Lin, C. Y., Macey, D. J., Austin, J. M., Jr., Kilgore, L. C., Grizzle, W. E., Schlom, J., and LoBuglio, A. F. Intraperitoneal radioimmunochemotherapy of ovarian cancer: A phase I study. Cancer Biother. Radiopharm., *16:* 305–315, 2001.
34. Knox, S. J., Goris, M. L., Tempero, M., Weiden, P. L., Gentner, L., Breitz, H., Adams, G. P., Axworthy, D., Gaffigan, S., Bryan, K., Fisher, D. R., Colcher, D., Horak, I. D., and Weiner, L. M. Phase II trial of yttrium-90-DOTA-biotin pretargeted by NR-LU-10 antibody/streptavidin in patients with metastatic colon cancer. Clin. Cancer Res., *6:* 406–414, 2000.
35. Barbet, J., Kraeber-Bodere, F., Faivre-Chauvet, A., Ferrer, L., Rousseau, C., Resche, I., Vuillez, J. P., Devillers, A., Chang, K., Sharkey, R. M., and Goldenberg, D. M. Pharmacokinetics and biodistribution of anti-CEA x anti-hapten bispecific antibody (BsMAb) and ^{131}I-labeled hapten in pretargeted radioimmunotherapy patients. J. Nucl. Med., *43:* 159p (abstract 579), 2002.
36. Trejtnar, F., Laznicek, M., Laznickova, A., and Mather, S. J. Pharmacokinetics and renal handling of ^{99m}Tc-labeled peptides. J. Nucl. Med., *41:* 177–182, 2000.
37. Moffatt, F., Pinsky, C. M., Hammerschaimb, L., Petrelli, N. J., Patt, Y. Z., Whaley, F. S., Goldenberg, D. M., and the Immunomedics Study Group. Clinical utility of external immunoscintigraphy with the IMMU-4 ^{99m}Tc antibody fragment (CEA-Scan^{TM}; arcitumomab) in patients undergoing surgery for carcinoma of the colon and rectum. J. Clin. Oncol., *14:* 2295–2305, 1996.
38. D. M. Goldenberg, H. A. Nabi, C. L. Sullivan, A. Serafini, D. Seldin, B. Barron, L. Lamki, B. Line, and W. A. Wegener: Carcinoembryonic antigen immunoscintigraphy complements mammography in the diagnosis of breast carcinoma. Cancer (Phila.), *89:* 104–115, 2000.
39. Klivényi, G., Schuhmacher, J., Patzelt, E., Hauser, H., Matys, R., Moock, M., Reigert, T., and Maier-Borst, W. Gallium-68 chelate imaging of human colon carcinoma xenografts pretargeted with bispecific anti-CD44$_{v6}$/antigallium chelate antibodies. J. Nucl. Med., *39:* 1769–1776, 1998.
40. Schuhmacher, J., Klivényi, G., Kaul, S., Henze, M., Matys, R., Hauser, H., and Clorius, J. Pretargeting of human mammary carcinoma xenografts with bispecific anti-MUC-1/anti-Ga chelate antibodies and immunoscintigraphy with PET. Nucl. Med. Biol., *28:* 821–828, 2001.
41. Sharkey, R. M., Goldenberg, D. M., Vagg, R., Pawlyk, D., Wong, G. Y., Siegel, J. A., Murthy, S., Levine, G. M., Izon, D., Gascon, P., Burger, K., Swayne, L. C., and Hansen, H. J. Phase I clinical evaluation of a new murine monoclonal antibody (Mu-9) against colon-specific antigen-p for targeting gastrointestinal carcinomas. Cancer (Phila.), *73:* 864–877, 1994.
42. Sharkey, R. M., Rossi, E., Karacay, H., McBride, W., Chang, K., Zang, L., Qu, T., Griffiths, G. L., Hansen, H. J., and Goldenberg, D. M. A novel, recombinant, bispecific antibody pretargeting system for cancer radioimmunotherapy. Clin. Cancer Res., *7:* 3786s, 2001.

A Universal Pretargeting System for Cancer Detection and Therapy Using Bispecific Antibody

Robert M. Sharkey, William J. McBride, Habibe Karacay, et al.

Cancer Res 2003;63:354-363.